Photocatalytic ozonation of pyridine-based herbicides by N-doped titania

Rafael R. Solís[a], F. Javier Rivas*, [a], Olga Gimeno[a], José Luis Pérez-Bote[b]

[a]Departamento de Ingeniería Química y Química Física. Universidad de Extremadura

Edificio Jose Luis Sotelo, Av. Elvas s/n 06006 Badajoz (Spain)

[b]Departamento de Anatomía, Biología Celular y Zoología. Universidad de Extremadura

Av. Elvas s/n 06006 Badajoz (Spain)

Abstract

BACKGROUND: A mixture of three pyridine herbicides in water (clopyralid, triclopyr and picloram) has been treated with photocatalytic processes, involving oxygen or ozone. Nitrogen doped and undoped titania were used in the process. Toxicity evolution during photocatalytic ozonation was monitored considering BOD, *Daphnia parvula* and fitotoxicity trials.

RESULTS: N doped titania with an optimized photoactivity was tested in photocatalytic ozonation, leading to nearly 95% of mineralization in 180 min. This catalyst was characterized by SEM, TEM, XRD and XPS techniques (13.5 nm of crystal size, anatase phase, 1% of N, and formation of O-Ti-N linkage). No loss of photocatalytic activity was appreciated after 5 consecutive runs. Although no toxicity from the parent compounds was observed, this parameter increased at the early stages of the oxidation process. When parent compounds were totally degraded and dechlorination was completed, toxicity decayed again to negligible values.

---

*Correspondence to: FJ Rivas, Departamento de Ingeniería Química y Química Física, Universidad de Extremadura, Avda. Elvas s/n, 06071, Badajoz (Spain). Email: fjrivas@unex.es, Phone 34 924289300, FAX 34 924289385

[a] Departamento de Ingeniería Química y Química Física, Universidad de Extremadura, Avda. Elvas s/n, 06071, Badajoz (Spain)

[b] Departamento de Anatomía, Biología Celular y Zoología. Universidad de Extremadura Av. Elvas s/n, 06071, Badajoz (Spain)

CONCLUSION: N doping improves bare titania photoactivity through an optimum of N amount. Photocatalysis/ozone showed better behavior than photocatalysis/oxygen in herbicide removal and mineralization, and no significant loss activity was appreciated after 5 runs. Toxicity initially increases due to toxic byproducts formation; however, it decreased after their abatement.

Keywords: Clopyralid, picloram, triclopyr, photocatalysis, photocatalytic ozonation, doped titania

INTRODUCTION

Picloram (4-amino-3,5,6-trichloro-2-pyridinecarboxylic acid), clopyralid (3,6-dichloro-2-pyridinecarboxylic acid) and triclopyr (3,5,6-trichloro-2-pyridinyloxyacetic acid) are selective herbicides included in the chlorinated pyridine derivatives family. Picloram and clopyralid belongs to the picolinic acid family while triclopyr derives from the pyridiniloxyacetic acid.

Picloram is used to kill unwanted broad-leaved plants on pastures and rangeland, in reforestation programs, in uncultivated areas, and along rights-of way, being majority used on pasture and rangeland.[1] In the case of clopyralid, it is used to kill unwanted annual and perennial broadleaf plants in turf and lawn, range, pasture, rights-of-ways, and some agricultural crops.[2] Pastures, woodlands, and rights of way are the main scenarios of triclopyr uses, while rice is the major agricultural one.[3]

The main concern related to the use and application of these herbicides is their relatively high solubility in water, persistence and mobility. Due to this, they are likely to leach groundwater or surface water which is certain in those areas where residues may be persistent in the overlying solid.[4-7] Once in water, the herbicides are unlikely to degrade even after a long period of time. Otherwise, special relevance is the potential carryover

of picolinic herbicides in animal manure, compost, plant mulch, etc. These species may pose phytotoxic properties for non-target plants after their uncontrolled applications. Some crops such as tomatoes, potatoes (picloram, clopyralid) or tobacco (picloram) are negatively affected by the exposure to these herbicides.

Efficient methodologies in water treatment to remove micro-contaminants involve physical processes such as adsorption on activated carbon, membrane technologies, or chemical stages such as oxidation/reduction processes. Amongst the latter, photocatalysis emerges as one of the most attractive technologies, especially when solar radiation or low cost radiation sources are used. Black light lamps are economical devices characterized by their emission in the proximity of 365 nm. Furthermore, they may be a suitable alternative in areas where climate limit the use of solar radiation. The correct selection of an active and stable photocatalyst is of paramount importance. Titanium dioxide is an economical and suitable choice due to its non-toxic nature and photocatalytic activity. Generation of the pair hole-electron is produced for wavelengths lower than 387 nm. Doping of TiO_2 can lead to an increase of the maximum wavelength excitation or, alternatively a higher quantum yield corresponding to a particular wavelength.

One of the reactions to be minimized in the photocatalysis is the recombination of electron-holes leading to the inefficient heat release. This step is partially prevented by the oxygen presence which is reduced while holes directly react with contaminants or with water to produce hydroxyl radicals. Trapping of electrons can also be accomplished by inorganic peroxides such as H_2O_2, monopersulfate, persulfate, etc.[8] A promising alternative is the simultaneous application of ozone and photocatalysis. This combination allows for the concurrent action of molecular ozone and photocatalysis with the synergistic effect of electron trapping by O_3. Electron trapping by ozone leads

to the development of a radical mechanism capable of generating more powerful hydroxyl radicals than the process in the presence of oxygen:[9]

$$TiO_2 + h\nu \rightarrow e^- + h^+ \quad (1)$$

$$\left.\begin{aligned} O_2 + e^- &\rightarrow O_2^{\bullet -} \\ O_3 + e^- &\rightarrow O_3^{\bullet -} \end{aligned}\right\} \text{Electron trapping} \quad (2)$$

$$\left.\begin{aligned} &O_2^{\bullet -} + H^+ \rightarrow HO_2^{\bullet} \xrightarrow{+HO_2^{\bullet}} O_2 + H_2O_2 \xrightarrow{+O_2^{\bullet -}} O_2 + HO\bullet + OH^- \\ &O_3^{\bullet -} + H^+ \rightarrow HO_3^{\bullet} \rightarrow O_2 + HO\bullet \\ &h^+ + H_2O_2 \rightarrow H^+ + HO\bullet \end{aligned}\right\} HO\bullet \text{ generation} \quad (3)$$

$$\left.\begin{aligned} e^- + R &\rightarrow \text{Products} \\ HO\bullet + R &\rightarrow \text{Products} \\ h^+ + R &\rightarrow \text{Products} \end{aligned}\right\} \text{Parent compounds initial abatement reactions} \quad (4)$$

In this work an attempt has been made to synthetize a TiO_2 based photocatalyst by improving its properties by means of nitrogen doping[10-14]. For that purpose, triethylamine was considered according to its higher capacity of forming a stable organic titanium complex which plays an important role during the hydrolysis stage (Yu et al., 2007).[15]

A mixture of picloram, clopyralid and triclopyr has been used to test the activity and stability of the catalyst. These herbicides have been eliminated from aqueous media by several technologies such as Fenton[16], electro Fenton[17], photo Fenton[18], O_3/H_2O_2[19], photocatalysis[20-24], UV[25] and H_2O_2/UV[26], etc. However, to the best of author´s knowledge, the efficiency of photocatalytic ozonation has not been investigated in the removal of pyridine-based herbicides.

EXPERIMENTAL

Photoreactor and procedure

A scheme of the experimental setup is shown in Figure 1. It is composed by a 1.0 L reactor inside an external cylinder pipe (54 cm of height and 31 cm of external diameter) with four black light lamps of 41 cm of length attached to the inner wall. The lamps (LAMP15TBL HQPOWERTM manufactured by Velleman®, 41 cm of length and 15 W of nominal power emitting in the range 350-400 nm) were equidistantly distributed at 90º. The inner wall was covered by aluminum foil to increase the photons reflection. Actinometry experiments in the presence of ferryoxalate led to the quantification of the radiation with a value of $6.86 \cdot 10^5$ Einstenin min^{-1} L^{-1} when the 4 lamps were in use.

The photoreactor was continuously fed with oxygen, nitrogen or a mixture of oxygen-ozone by means of a diffuser placed inside the reaction bulk. 30 L h^{-1} gas flow rate was used in all trials. The solid photocatalysts were added before the photoreaction to reach the herbicides adsorption equilibria onto their surface. When samples were extracted, the solid was removed by filtration through Millex-HA filters (Millipore, 0.45 μm).

Ozone was produced by electrical decomposition of oxygen in a Sander Laboratory Ozone Generator. Ozone gas phase concentration was monitored by an Anseros Ozomat ozone analyzer.

Materials

Pure herbicides, titanum (IV) isopropoxide (97%) and potassium indigotrisulfonate were purchased from Sigma-Aldrich; while triethylamine (99.5%), hydrochloride acid (37%) and absolute ethanol were from Panreac. HPLC was fed with organic solvents from VWR Chemicals and ionic chromatography solutions were prepared with Sigma-

Aldrich reagents. All chemicals were used as received. Finally, water from a Mili-Q water system (Millipore) was used for preparation of all solutions and suspensions.

N-doped titania synthesis

The lab-made photocatalysts were synthesized applying a sol-gel method followed by thermal treatment and calcination. Some literature methodology was carried out in order to synthesize them[27]. Roughly, it starts with the dissolving of titanium isopropoxidde in ethanol and the following addition of a determined amount of the nitrogen organic source (in this case triethylamine), to meet the required N:Ti ratio. Afterwards, HCl 0.1 was gradually added to the organic solution to get a clear liquid. Precipitation process was completed by autoclaving the mixture at 80 ºC for 12 hours. Then, the suspension was centrifuged at 3500 rpm, and the resultant solid was dried overnight at 100 ºC. Finally, calcination was carried out at 500 ºC for 4 hours with an initial ramp of 10 ºC min^{-1}. The manufacturated photocatalysts were labeled with the general formula TiO_2_1:x. In this nomenclature, 1:x means the ration of Ti atoms to N atoms in the synthesis process.

Catalyst characterization

X-ray Photoelectron Spectroscopy (XPS) spectra was conducted in a XPS K-alpha-Thermo Scientific equipment, working with a Kα monochromatic source of Al (1486.68 eV). A value of 284.8 eV for the C 1s peak was taken to calibrate the signals of Ti 2p, O 1s, N 1s peaks. Crystalline phase were analyzed by X Ray Diffraction (XRD), in a Bruker D8 ADVANCE diffract meter equipped with a monochromator of Ge 111 Kα of Cu (wavelength, 1.5456 Å). Transmission Electron Microscopy (TEM) analysis was applied by a TEM Tecnai G2 20 Twin-FEI Company apparatus (filament LaB_6, voltage 200 KV, magnification up to $1.05x10^6$) while Scanning Electron Microscopy (SEM)

was conducted in a HITACHI S-4800 coupled to a secondary electrons detector (acceleration voltage 20 kV).

Diffuse reflectance UV–VIS spectroscopy, used to obtain the catalysts UV-VIS absorbance spectra and their band gap values, were completed with a Jasco V670 UN/VIS/NIR spectrophotometer equipped with an integrating sphere device.

BET surface area was quantified trough nitrogen adsorption isotherms obtained at 77 K with a Quadrasorb instrument (Quantachrome). Samples were treated previously at 150 ºC for 24 h under high vacuum conditions for outdegassing the adsorbed gases.

Thermal gravimetry, differential temperature analysis and released gases mass spectrometry (TG-DTA-MS) were performed with a Setaram SETSYS Evolution-16 equipment connected to a PrismaTM QMS200 quadrupole mass spectrometer. The operation conditions were: sample loading 28 mg, air flow rate 50 mL min^{-1} and heating rate of 10 °C min^{-1} from room temperature to 900 °C.

Analysis

High Performance Liquid Chromatography (Agilent 1100) was used in the analysis of herbicides. The HPLC was equipped with a Kromasil 100 5C18 column. A gradient elution was pumped at a flow rate of 1 mL min^{-1}, and the acetonitrile: acidified water (0.1% H_3PO_4) volume percentages were increased from 10:90 to 50:50 in 12 minutes. After that, it was kept in 50:50 for 6 minutes. An engaged wavenumber of 230 nm was considered for conduction.

Short chain organic and inorganic anionic compounds were monitored by ionic chromatography (Metrohm 881 Compact Pro). Total Organic Carbon (TOC) content was determined by means of a Shimazdu TOC 5000A analyzer which directly injects the aqueous sample.

159 The method based on the decoloration of the 5,5,7-indigotrisulfonate was applied for
160 the determination of dissolved ozone concentration in aqueous solution.[28]

161 A GLP 21+ CRISON pH-meter was used for pH measures. pH of the media was not
162 adjusted and reaction was conducted at the natural pH after herbicides addition. In
163 toxicity trials, pH was adjusted with H_3PO_4 and NaOH.

164 Biological oxygen demand after five days (BOD_5) was conducted by respirometry.
165 Commercial respirometers OXITOP® were used for that purpose. BOD_5 was
166 determined after addition of some inorganic salts, nutrients and microorganisms from
167 activated sludge to simulate the behavior in a standard residual urban wastewater. A
168 synthetic wastewater representing a secondary treated effluent was artificially
169 prepared[29]. Inoculate was obtained from the local wastewater treatment plant of the city
170 of Badajoz.

171 **Ecotoxicity bioassays with *Daphnia parvula***

172 For ecotoxicity purposes, the acute toxicity to *Daphnia parvula* was carried out
173 according to US EPA standard procedure.[30] The crustaceans were grown up in artificial
174 ponds located at Extremadura University installations.

175 The analysis started placing 20 second instar *D. parvula* into a 100 mL of water sample,
176 by means of disposable plastic transfer pipettes. After that, the crustaceans were
177 exposed to 16:8 light: dark photoperiods at room temperature. Survival organisms were
178 counted at 24 and 48 hours, without being fed. The herbicides were dissolved in mineral
179 water (composition: 10.7 mg L^{-1} HCO_3^-, 5.3 mg L^{-1} SO_4^{2-}, 19.0 mg L^{-1}, Cl^-, 2.7 mg L^{-1},
180 Ca^{2+} 2.7 mg L^{-1} Mg^{2+}, 14.7 mg L^{-1}, Na^+, and 14.3 mg L^{-1} SiO_2). In these experiments,
181 pH was adjusted to 7 ± 0.1 after extracting samples. Three blank samples without
182 herbicide addition were considered in order to study the mortality due to natural

183 reasons. One photocatalytic ozonation process was carried out; samples at different
184 stages of oxidation extent of the most refractory herbicide were extracted (0, 25, 50, 75,
185 and 100% of initial CLO removal). A final sample when TOC removal achieved a
186 steady state level was also analyzed.

187 The formula proposed by Abbott was used to correct the survival percentage due to
188 natural causes:[31]

189 $$\%\,M'_S = \frac{\%\,M_S - \%\,M_B}{100 - \%\,M_B} \quad (5)$$

190 $$\%\,S'_S = 100 - \%M'_S \quad (6)$$

191 In these equations M_S and M_B stands for mortality without correction in the sample and
192 blank tests, respectively; and, M'_S and S'_S are the sample respective mortality and
193 survival corrected percentages.

194 **Acute fitotoxicity assay**

195 Seeds of *Lactuca Sativa* and *Solanum Lycopersicum* were purchased from Vilmorin®
196 (Batavia blonde of Paris lettuce and cherry tomato respectively) and used as test plants
197 for acute fitotoxicity assays of water samples extracted at different times of o treatment.

198 Fifty *L. Sativa* or *S. Lycopersicum* seeds were equally distributed into Petri dishes
199 equipped with paper discs moistened with 4 mL of water sample. The dishes were
200 covered with paraffin plastic in order to avoid liquid evaporation, and incubated in a
201 germination chamber isolated from light at 22 ± 2 ºC for 120 hours. After that period,
202 the root length (L), expressed as the sum of hypocotyl and radicle, was measured for
203 those seeds whose germination had taken place.

Additionally, a negative control or blank of MiliQ® water and a positive control of H_2O_2 300 mM were carried out. The validity criteria for the test were an upper 90% of germination and a variation coefficient for the root growth below 30% in negative control experiments. Positive control led to germination of none of the seeds. The percentage root growth was calculated by comparing the radicle lengths for each sample with those observed in the control (L/L_{Blank}).

RESULTS AND DISCUSSION

Photocatalytic oxidation. Activity of catalyst with different Ti:N ratios

Previously to the application of ozone, some photocatalytic tests were carried out in the presence of oxygen. Different catalysts were synthetized by varying the ratio Ti:N in the manufacturing process. Accordingly, different doping percentages are expected in the lab made photocatalysts. Doping percentage of titania particles influences the activity of the photocatalyst.[32] Hence, Ti:N ratios from 1:0 to 1:2 were used in the photocatalysis of a mixture of the three herbicides considered in this work.

Figure 2 shows the evolution of the normalized concentration of herbicides treated in the presence of different catalysts. Also, the evolution of total organic carbon (TOC) is displayed.

The positive effect of N-doping is observed in Fig. 2. Regardless of the catalyst nitrogen content, the presence of this anionic dopant improves the conversion of the herbicides and the mineralization degree achieved after 180 min of treatment. An optimum in N percentage was experienced when the TiO_2_1:1.6 catalyst was used. The presence of an optimum relies on the influence of opposite effects. On one hand, N doping involves a decrease in the band gap energy and, as a consequence, a higher photolytic activity. On the other hand, an increase in diameter particle (lower specific area), formation of TiN

(non-transparent), and the amount of oxygen vacancies (electron –hole recombination sites) are related to high N doping photocatalysts.[33] In any case, this subject is somehow controversial. Hence, some authors claim that N doping decreases particle size while electron hole recombination is prevented by oxygen vacancies (photoluminescence intensity minimization)[34] An increase in BET surface area as N percentage reaches a determined value has been reported, values above the optimum lead to a BET area decrease.[35]

The mechanisms of improved photoactivity of N doped titania are out of the scope of this work.

Under optimum conditions, after 3 hours of reaction, mineralization of the herbicides was 50%. Therefore, in an attempt to improve the TOC conversion extent, the photocatalysis was carried out in the presence of ozone, leading to the photocatalytic ozonation process. For comparison purposes, single ozonation was first applied.

Ozonation and photocatalytic ozonation. Activity of catalyst with different Ti:N ratios

Ozonation of the herbicides mixture (Fig. 3) confirms the recalcitrant nature of these compounds towards molecular ozone. In fact, in a previous work the rate constants between ozone and the herbicides were tested and took values of $20\,M^{-1}\,min^{-1}$ for clopyralid and triclopyr, and $105\,M^{-1}\,min^{-1}$ in the case of picloram.[36] TOC nearly remains constant showing conversion values in the proximity of 10% after 3 hours of ozonation. Dissolved ozone and at the reactor outlet were immediately detected and remained unchanged throughout the process, corroborating the slow regime developed in this heterogeneous reaction. Accordingly, the system UVA/O_3/TiO_2 1:x was applied by using different TiO_2_1:x catalysts.

Figure 3 shows the results obtained in photocatalytic ozonation experiments. As observed, use of ozone in the presence of titania significantly increases the efficiency of herbicides removal and TOC conversion. In this case, however, with the exception of the TiO_2_1:1.6 catalysts, doping of titania particles does not necessarily enhance the abatement rate of herbicides. Moreover, TiO_2_1:0.8 and TiO_2_1:2.0 display a worse performance than undoped TiO_2_1:0 when herbicides conversion is monitored. The best results, in terms of parent compounds elimination, were experienced with the TiO_2_1:0.4 and TiO_2_1:1.6 catalysts. These two catalysts are capable of achieving >99% conversion of clopyralid, picloram and triclopyr in 60, 20 and 30 min, respectively. After 180 min, single ozonation just led to 27, 77, and 44% conversion of the same herbicides. Again, it seems that an optimum in N doping extent does exist. Mineralization of the reaction mixture revealed the higher activity of TiO_2_1:1.6 if compared to the rest of catalysts and, obviously, to single ozonation. For instance, photocatalytic ozonation in the presence of TiO_2_1:1.6 led to 80% mineralization in roughly 60 min, while the rest of tested catalyst required 180 min on average to achieve the same TOC conversion.

Photocatalytic ozonation in the presence of undoped titania suggests the existence of some synergistic effect when combining the UVA/TiO_2_1:1.0 and O_3 systems. This synergism is particularly visible when TOC evolution is analyzed. Hence, the UVA/TiO_2_1:1.0 system hardly achieved 5% in TOC reduction while single ozonation just led to 10% of mineralization (after 180 min). Adding up the TOC conversion experienced in individual systems (roughly 15%) is far away from 80% obtained in the combined process. As stated previously, doping of the titania particles to generate the TiO_2_1:1.6 catalyst rose the final TOC removal up to 95% after 180 min of treatment. Synergism is also observed with the later catalyst, experiencing TOC reductions of 10%

277 and 45% corresponding to single ozonation and photocatalytic oxidation respectively
278 after 3 hours.

279 **Photocatalytic ozonation. Stability and characterization of TiO_2_1:1.6 catalyst.**

280 Stability of the TiO_2_1:1.6 catalyst (the most active solid) was assessed by recycling the
281 solid through five consecutive runs with no replacement of solid losses during the
282 recovery stages.

283 Recovery of the catalyst by filtration at lab scale led to significant reductions in the
284 catalyst amount used in the following run. Thus, catalyst concentration in the 2^{nd}, 3^{rd},
285 4^{th}, and 5^{th} runs were reduced to 66%, 46%, 30% and 20% of the amount used in the 1^{st}
286 experiment. As inferred from Fig. 4, a slight decrease in herbicide removal rate was
287 experienced after the 2^{nd} use. However, this fact was not impediment to achieve 100%
288 conversion of the parent compounds at similar reaction times than those obtained in the
289 first two runs. Analogous behavior was observed when TOC conversion was
290 considered. Hence, mineralization of the mixture in the range 90-95% was obtained
291 after 180 min regardless of the amount of the catalyst and reuse. For comparison
292 purposes an empirical pseudo first order reaction constant has been calculated and
293 normalized to the catalyst concentration used in each run. Hence, the normalized rate
294 constants were 0.053, 0.089, 0.0767, 0.10 and 0.14 min^{-1} L g^{-1}, corresponding to the
295 first, second, third, fourth and fifth reuses, respectively. These empirical reaction rates
296 have revealed that effectively no apparent deactivation of the catalyst occurs, moreover,
297 some enhancement of the process can be envisaged likely due to an optimization in
298 catalyst concentration in the media. Some theoretical analysis of the reactor geometry
299 and efficiency based on Monte Carlo simulations reveal that optimum catalyst

300 concentration is even below 0.1 g/L to achieve the maximum LVRPA (local volumetric
301 rate of photon absorption).

302 To elucidate the possible reason for the TiO_2_1:1.6 higher activity, some preliminary
303 tests were applied to all the manufactured solids. UV-vis absorption spectra profiles of
304 manufactured catalysts are shown in figure 5. This figure reveals no significant
305 differences in the obtained spectra. Tauc´s method to calculate the band gap energy was
306 thereafter applied[37]. Table 1 displays the results obtained, confirming that the band gap
307 energy of the solids were quite similar and do not explain the observed differences in
308 activity.

309 The other parameter that has been suggested to contribute to the activity of N doped
310 titania is the increase in surface area. Table 1 shows the BET area found in nitrogen
311 adsorption experiments. At the sight of the displayed results, it is observed a higher area
312 of the TiO_2_1:1.6 catalyst that would explain its higher activity[35].

313 Given the high stability and activity of the TiO_2_1:1.6 catalyst, additional
314 characterization of this solid was carried out by different techniques. Figure 6 shows the
315 XRD pattern of TiO_2_1:1.6 as a function of temperature. As expected, according to the
316 temperature of calcination (500 ºC), a 100% anatase phase diphractogram was obtained.
317 Higher temperatures involves the partial transformation of anatase to the non-
318 photoactive rutile[32], hence, rutile percentages of 9.4, 15.3 and 24.3% where obtained at
319 temperatures of 550, 600 and 700 ºC, respectively. Scherrer equation was used to
320 estimate the crystal size (D) according to:

321 $$D = 0.9\frac{\lambda}{\beta \cos\theta} \qquad (7)$$

where θ is the diffraction angle of the peak selected, β the half height peak's width (in radians), λ the wavelength of the source of X ray applied (1,5456 Å for Cu radiation), K the Scherrer's constant which depends on the shape of the particles (value of 0.9 if spherical shape is considered). Considering the anatase peak at 2θ = 25.4º a value in the proximity of 13-14 nm was obtained in all diphractograms with the exception of 700 ºC where a higher value of 29 nm was obtained.

Three areas of the XPS spectrum were investigated: the Ti 2p , O 1s and N 1s regions (fig 7). The binding energy of N 1s when introduced into the TiO_2 structure extends from 397 to 403 eV. In the spectra of TiO_2_1:1.6, a peak at 400.0 eV is observed. 15s of sputtering led to the cleaning of the superficial layer and the energy of N 1s peak increased to 400.5 eV. According to literature, this peak can be attributed to the environment O-Ti-N[33], or the states of nitrogen doped in titania might be various and coexist the form N-Ti-O and Ti-O-N.[27] O 1s shows certain asymmetry due the fact that has contributions of two peaks, located at 530 and 531 eV. The first one is characteristic of O-Ti-O linkages, while the second one is frequently attributed to O-Ti-N structure.[38] Ti 2p peak observed (results not shown) had a lower binding energy compared to O-Ti-O linkage, which is also indicative of insertion of N in the TiO_2 lattice. Nitrogen content calculated from the spectra revealed values of 1.7 and 0.96%, before and after 15 s etching respectively. Shirley method was applied in order to determinate the baseline of quantified peaks.

SEM analysis of TiO_2_1:1.6 shows (fig. 8) a variety of particle sizes and shapes forming heterogeneous agglomerates. TEM images (fig. 8) corroborate the crystal size obtained by XRD. Some images display crystals showing an octahedral derived shape with the appearance of rhombic {100} and hexagonal {112} faces.

346 TG-DTA-MS

347 Figure 9 displays the percentage of mass loss in the characterization run. A linear
348 decrease is experienced up to 500 ºC. Thereafter a partial stabilization was observed.
349 The mass loss was roughly 24%. The differential thermal analysis reveals two main
350 exothermic variations in energy coinciding with the release of water and carbon dioxide
351 (280 and 440 ºC)

352 **Photocatalytic ozonation. Toxicity and fitotoxicity of treated samples.**

353 Toxicity of the herbicide mixture after photocatalytic ozonation was firstly tested by
354 monitoring BOD evolution of different samples.

355 BOD tests were carried out by using synthetic water doped with the herbicides and
356 being exposed to the photocatalytic ozonation process. Figure 10A shows the results.
357 BOD evolution of synthetic water, with and without doping before being treated by
358 photocatalytic ozonation, showed similar trends with a value after 5 days of 19 mg L^{-1}.
359 This might be indicative of the non-toxic nature of the herbicides. Nevertheless,
360 different results were observed after treating the initial compounds by the oxidation
361 process. After 10 minutes of treatment, parent compounds are completely abated; and,
362 BOD_5 dropped off to a value of 13 mg L^{-1} which could be considered as an increase in
363 toxicity. This effect is supposed to be due to the formation of reaction intermediates
364 more toxic than the parent compounds. Maximum in concentration of organic short
365 chain acids such as acetic, propionic and oxalic acids were detected (embedded figure of
366 plot in Fig. 10C). Rupture and opening ring of the herbicides take place at the early
367 stage of the process. Chloride profile sustains the previous hypothesis (embedded figure
368 of plot in Fig. 10B). After enough time of treatment (180 min), TOC removal reaches a

state value. At this point BOD_5 took a value of 17 mg L^{-1}, higher than BOD_5 at 10 minutes, but lower than the initial value (19 mg L^{-1}).

Since BOD is a general parameter affected by a number of variables, some additional toxicity tests by considering the exposure of *D. parvula* were completed. In this case, more samples at initial stages of parent herbicides oxidation were taken and exposed to the crustacean. The first one, which corresponds to a 25% removal of the most recalcitrant herbicide (clopyralid), showed the highest mortality rate. After that, survival rate increases to almost 100% in the sample of 75% clopyralid removal, and remains constant for the rest of the treatment. Again, as BOD_5 suggested previously, a maximum of toxicity appears at the early stage of the photocatalytic ozonation process. Formation of more toxic chloride organic intermediates before the dechlorination to short-chain organic compounds can explain the results. Once the herbicides have been degraded, mortality drops off to a negligible value. It should be highlighted that this absence of toxicity is in correspondence to mineralization extent, up to 95%.

Similar results to those previously discussed were found when fitotoxicity assays were completed (Figure 10D).

CONCLUSIONS

From the results extracted from this work, the following conclusions can be withdrawn:

- An optimum amount of triethylamine applied in the synthesis led to the highest activity in photocatalytic oxidation trials. N doping improves titania photoactivity.
- Photocatalytic ozonation considerably improved the herbicide and TOC abatement compared to photocatalytic oxidation or single ozonation..

- N doped titanium dioxide with the best photocatalytic behavior showed a 100% of anatase phase with a crystal size of 13.5 nm. XPS analysis suggests the formation of O-Ti-N linkage and N content of 1%.
- Photoactivity is maintained after four consecutive runs.
- At the early stages of the herbicide photocatalytic ozonation process, toxicity suffered a significant increase. It disappears when parent herbicides are completely abated and dechlorination is completed.

ACKNOWLEDGEMENTS

The authors thank the economic support received from Gobierno de Extremadura and CICYT of Spain through Projects GRU10012 and CTQ2012-35789-C02-01, respectively. Mr. Rafael Rodríguez Solís thanks Gobierno de Extremadura, Consejería de Empleo, Empresa e Innovación, and FSE Funds for his Ph.D. grant (PD12058).

REFERENCES

1 Cox C, Picloram herbicide factsheet, *J Pestic Reform* **18**:13-20 (1998).

2 Cox C, Clopyralid herbicide factsheet, *J Pestic Reform* **18**:15-19 (1998).

3 Cox C, Triclopyr herbicide factsheet, *J Pestic Reform* **20**:12-29 (1998).

4 Pang L, Close ME, Watt JPC, Vincent KW, Simulation of picloram, atrazine, and simazine leaching through two New Zealand soils and into groundwater using HYDRUS-2D. *J Contam Hydrol* **44**:19-46 (2000).

5 Liu L-C, Dumas JA, Cacho CL, Picloram groundwater contamination from pasture use. *J Agric Univ P R* **81** (1997).

6 Elliott JA, Cessna AJ, Nicholaichuk W, Tollefson LC, Leaching rates and preferential flow of selected herbicides through tilled and untilled soil. *J Environ Qual* **29**:1650-1656 (200).

415 7 Diaz R, Loague K, Assessing the potential for pesticide leaching for the pine forest
416 areas of Tenerife. *Environ Toxicol Chem* **20**:1958-1967 (2011).
417 8 Rivas J, Gimeno G, Borralho T, Carbajo M, UV-C photolysis of endocrine
418 disruptors. The influence of inorganic peroxides. *J Hazard Mater* **174**:393-397
419 (2010).
420 9 Agustina TE, Ang HM, Vareek VK, A review of synergistic effect of photocatalysis
421 and ozonation on wastewater treatment. *J Photochem Photobiol C* **6**: 264–273
422 (2005).
423 10 Fisher MB, Keane DA, Fernández-Ibánez P, Colreavy J, Hinder SJ, McGuigan KG,
424 Pilla SC, Nitrogen and copper doped solar light active TiO_2 photocatalysts for water
425 decontamination. *Appl. Catal. B: Environ*. **130– 131**: 8– 13 (2013).
426 11 Pelaez M, Cruz AA, Stathatos E, Falaras P, Dionysiou DD, Visible light-activated N-
427 F-codoped TiO_2 nanoparticles for the photocatalytic degradation of microcystin-LR
428 in water. *Catal . Today* **144**: 19–25 (2009).
429 12 Choi H, Antoniou MG, Pelaez M, Cruz AA, Shoemaker JA, Dionysiou DD,
430 Mesoporous Nitrogen-doped TiO_2 for the Photocatalytic Destruction of the
431 Cyanobacterial Toxin Microcystin-LR under Visible Light. *Environ. Sci. & Technol*.
432 **41 (21)**: 7530-7535 (2007).
433 13 Sacco O, Vaiano V, Han Ch., Sannino D, Dionysiou DD, Photocatalytic removal of
434 atrazine using N-doped TiO_2 supported on phosphors. *Appl. Catal. B: Environ.* **164**:
435 462–474 (2015).
436 14 Vaiano V, Sacco O, Sannino D, Ciambelli P, Photocatalytic removal of spiramycin
437 from wastewater under visible light with N-doped TiO_2 photocatalysts. *Chem. Eng.*
438 *J.* **261**: 3–8 (2015).

15 Yu J, Wang J, Zhang J, He Z, Liu Z, Ai X, Characterization and photoactivity of TiO_2 sols prepared with triethylamine. *Mater Lett* **61**:4984–4988 (2007).

16 Westphal K, Saliger R, Jäger D, Teevs L, Prüße U, Degradation of clopyralid by the Fenton reaction. *Ind Eng Chem Res* **52**:13924–13929 (2013).

17 Özcan A, Şahin Y, Koparal AS, Oturan MA, Degradation of picloram by the electro-Fenton process. *J Hazard Mater* **153**:718-727 (2008).

18 Huston PL, Pignatello JJ, Degradation of selected pesticide active ingredients and commercial formulations in water by the photo-assisted Fenton reaction. *Water Res* **33**:1238-1246 (1999).

19 Rudyak SS, Solozhenko EG, Soboleva NM, Goncharuk VV, Destruction of picloram under the effect of ozone and hydrogen peroxide. *Sov J Water Chem Tech* **9**:34-37 (1987).

20 Abramović B, Šojića D, Despotovića V, Vioneb D, Pazzib M, Csanádia J, 2011. A comparative study of the activity of TiO_2 Wackherr and Degussa P25 in the photocatalytic degradation of picloram. *Appl Catal B: Environ* **105**:191-198 (2011).

21 Poulios I, Kositzi M, Kouras A, Photocatalytic decomposition of triclopyr over aqueous semiconductor suspensions. *J Photochem Photobiol A: Chem* **115**:175-183 (1998)

22 Qamar M, Muneer M, Bahnemann D, Heterogeneous photocatalysed degradation of two selected pesticide derivatives, triclopyr and daminozid in aqueous suspensions of titanium dioxide. *J Environ Manag* **80**:99-106 (2006).

23 Šojić DV, Anderluh VB, Orčić DZ, Abramović BF, Photodegradation of clopyralid in TiO_2 suspensions: Identification of intermediates and reaction pathways. *J Hazard Mater* **168**:94-101 (2009).

463 24 Šojić D, Despotović V, Abramović B, Todorova N, Giannakopoulou T, Trapalis C,
464 Photocatalytic degradation of mecoprop and clopyralid in aqueous suspensions of
465 nanostructured N-doped TiO_2. *Molecules* **15**:2994-3009 (2010).
466 25 Orellana-García F, Álvarez MA, López-Ramón V, Rivera-Utrilla J, Sánchez-Polo M,
467 Mota AJ, Photodegradation of herbicides with different chemical natures in aqueous
468 solution by ultraviolet radiation. Effects of operational variables and solution
469 chemistry. *Chem Eng J* **255**:307-315 (2014).
470 26 Tizaoui C, Mezughi K, Bickley R, 2011. Heterogeneous photocatalytic removal of
471 the herbicide clopyralid and its comparison with UV/H_2O_2 and ozone oxidation
472 techniques. *Desalin* **273**:197-204 (2011).
473 27 Senthilnathan J, Philip L, Photocatalytic degradation of lindane under UV and visible
474 light using N-doped TiO_2. *Chem Eng J* **161**:83-92 (2010).
475 28 Bader H, Hoigné J, Determination of ozone in water by the indigo method. *Water*
476 *Res* **15**:449-456 (1981).
477 29 Erdei L, Arecrachakul N, Vigneswaran S, A combined photocatalytic slurry reactor-
478 immersed membrane module system for advanced wastewater treatment. *Sep Purif*
479 *Technol* **62**:382-388 (2008).
480 30 EPA, 2002. Methods for measuring the acute toxicity of effluents and receiving
481 water to freshwater and marine organisms. 5th edition, Washington.
482 31 Abbott WS, A method of computing the effectiveness of an insecticide. *J Econ*
483 *Entomol* **18**:265-267 (1925).
484 32 Carp O, Huisman CL, Reller A, Photoinduced reactivity of titanium dioxide. *Prog*
485 *Solid State Chem* 32:33-177 (2004)

33 Cha J-A, An S-H, Jang H-D, Kimc C-S, Song D-K, Kim T-O, Synthesis and photocatalytic activity of N-doped TiO_2/ZrO_2 visible-light. *Adv Powder Tech* **23**:717-723 (2012).

34 Cong Y, Zhang J, Chen F, Anpo M, Synthesis and characterization of Nitrogen-doped TiO_2 nanophotocatalyst with high visible light activity. *J Phys Chem C* **111**:6976-6982 (2007).

35 Dhanya TP, Sugunan S, Preparation, Characterization and Photocatalytic Activity of N doped TiO_2. *IOSR J Appl Chem* **4**:27-33 (2013).

36 Solís RR, Rivas FJ, Gimeno O, Pérez-Bote JL, Photocatalytic ozonation of clopyralid, picloram and triclopyr. Kinetics, toxicity and operational parameters influence. *J Chem Technol Biotechnol* DOI: 10.1002/jctb.4542 (2014).

37 Tauc J, Grigorovici R, Vancu A, Optical Properties and Electronic Structure of Amorphous Germanium. *Phys. Stat. Sol*.**15**:627-637 (1966).

38 Chen X, Burda C, Photoelectron spectroscopic investigation of nitrogen-doped titania nanoparticles. *J Phys Chem B* **108**:15446-15449 (2004).

502 **Table 1.** Characterization of manufactured catalysts.

Catalyst	BG (eV)	S_{BET} (m^2/g)
TiO_2_1:0	2.991	14.48
TiO_2_1:0.4	3.145	-
TiO_2_1:0.8	3.095	11.34
TiO_2_1:1.2	3.129	-
TiO_2_1:1.6	3.130	34.56
TiO_2_1:2.0	3.075	12.98

503

504

505

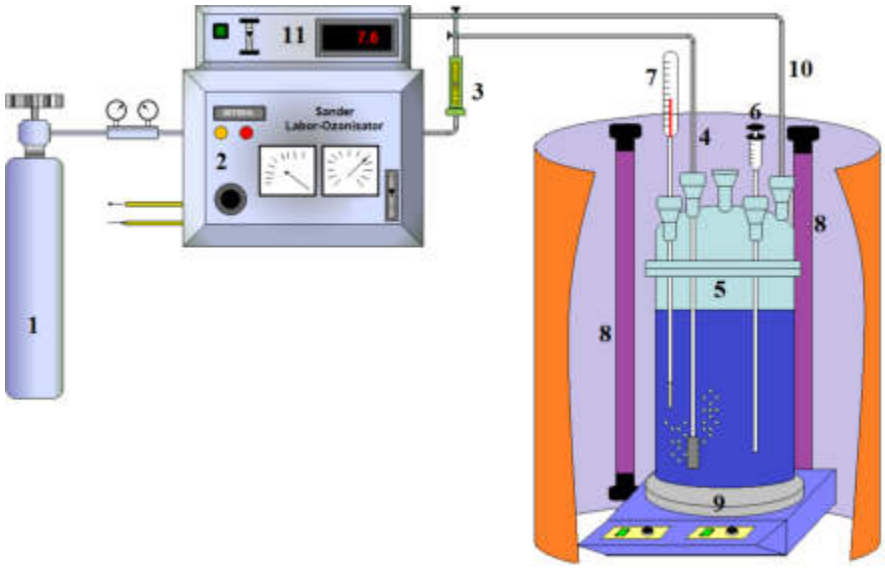

Figure 1. Experimental setup: 1, oxygen; 2, ozone generator; 3, flow rate controller; 4, gas inlet; 5, cylindrical reactor; 6, sampling port; 7, thermometer; 8, black-light lamps; 9, magnetic stirrer; 10, gas outlet; 11, ozone analyzer.

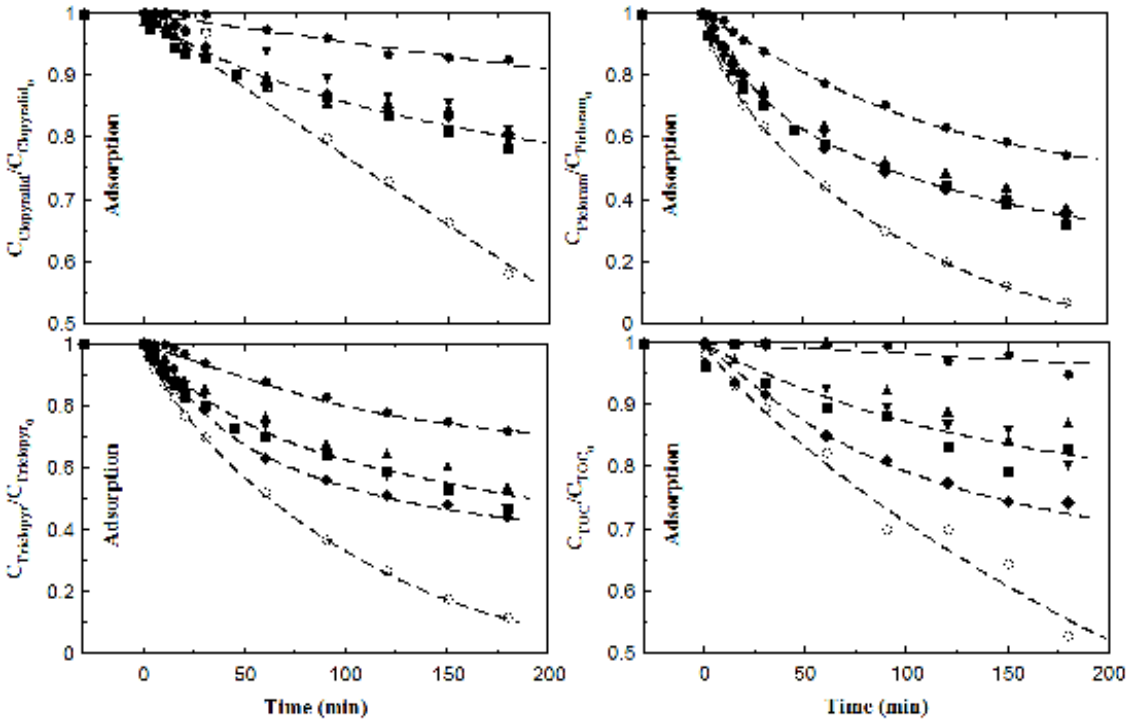

Figure 2. Black light photocatalysis of a mixture of clopyralid, picloram and triclopyr. Experimental conditions: T = 20 ºC, V = 1.0 L; I = $6.86 \cdot 10^{-5}$ Einstein min^{-1} L^{-1}; pH = 4.0 (average value), $C_{herbicide}$ = 5.0 ppm (each), $C_{Catalyst}$ = 0.5 g L^{-1}. Catalyst: ●, TiO_2_1:0; ■, TiO_2_1:0.4; ▲, TiO_2_1:0.8; ▼, TiO_2_1:1.2; o, TiO_2_1:1.6; ♦, TiO_2_1:2.

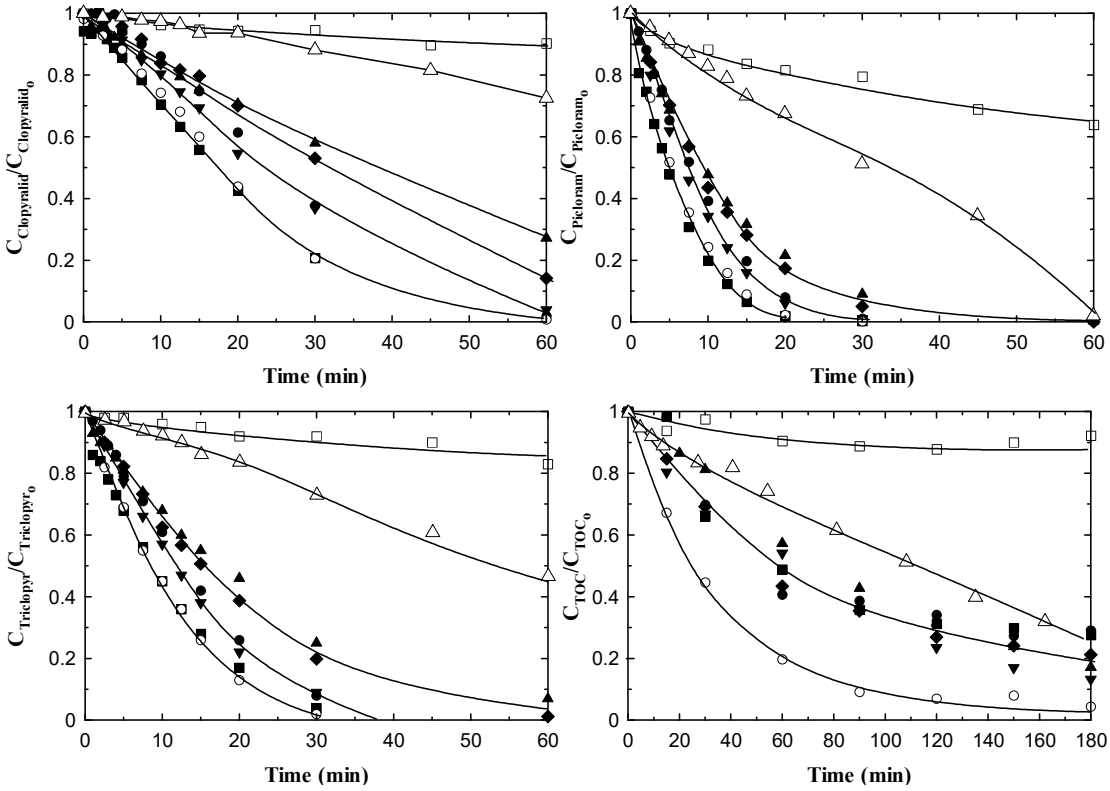

Figure 3. Black light photocatalytic ozonation of a mixture of clopyralid, picloram and triclopyr. Experimental conditions: T = 20 ºC, V = 1.0 L; I = $6.86 \cdot 10^{-5}$ Einstein min^{-1} L^{-1}; pH = 4.0 (average value), $C_{herbicide}$ = 5.0 ppm (each), $C_{Catalyst}$ = 0.5 g L^{-1}. □, Single ozonation; Δ, Photolytic ozonation; Photocatalytic ozonation: Catalyst: ●, TiO_2_1:0; ■, TiO_2_1:0.4; ▲, TiO_2_1:0.8; ▼, TiO_2_1:1.2; o, TiO_2_1:1.6; ♦, TiO_2_1:2.

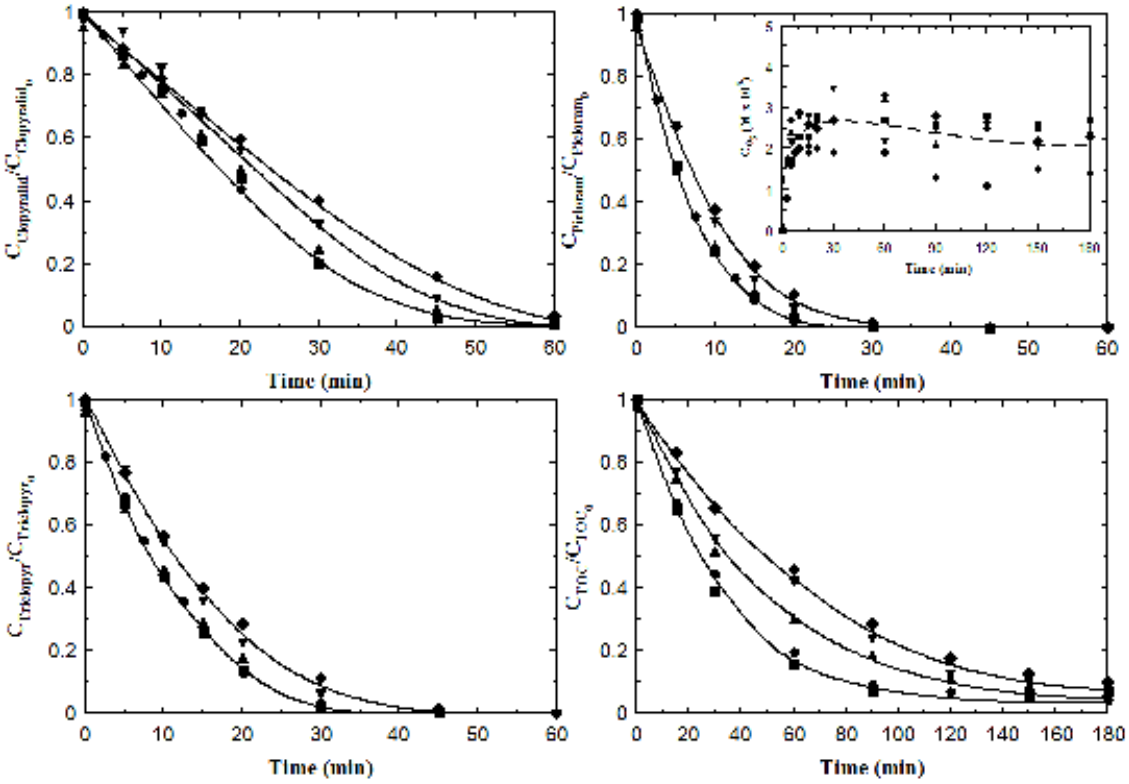

Figure 4. Black light photocatalytic ozonation of a mixture of clopyralid, picloram and triclopyr. Experimental conditions: T = 20 ºC, V = 1.0 L; I = $6.86 \cdot 10^{-5}$ Einstein min^{-1} L^{-1}; pH = 4.0 (average value), $C_{herbicide}$ = 5.0 ppm (each). $C_{Catalyst}$= TiO_2_1:1.6 (g L^{-1}): ●, 0.50 1st use; ■, 0.33 2nd use; ▲, 0.23 3rd use; ▼, 0.15 4th use; o, ♦, 0.10 5th use.

1

2

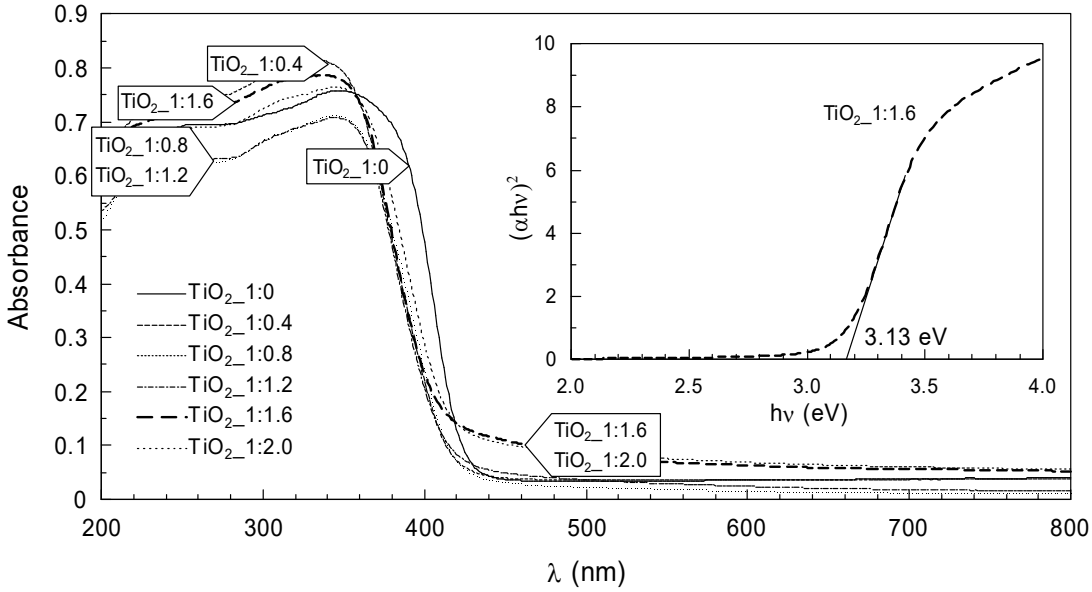

Figure 5. UV-vis absorption spectra profiles of catalysts and Tauc's plot corresponding to TiO_2_1:1.6 (inlet figure).

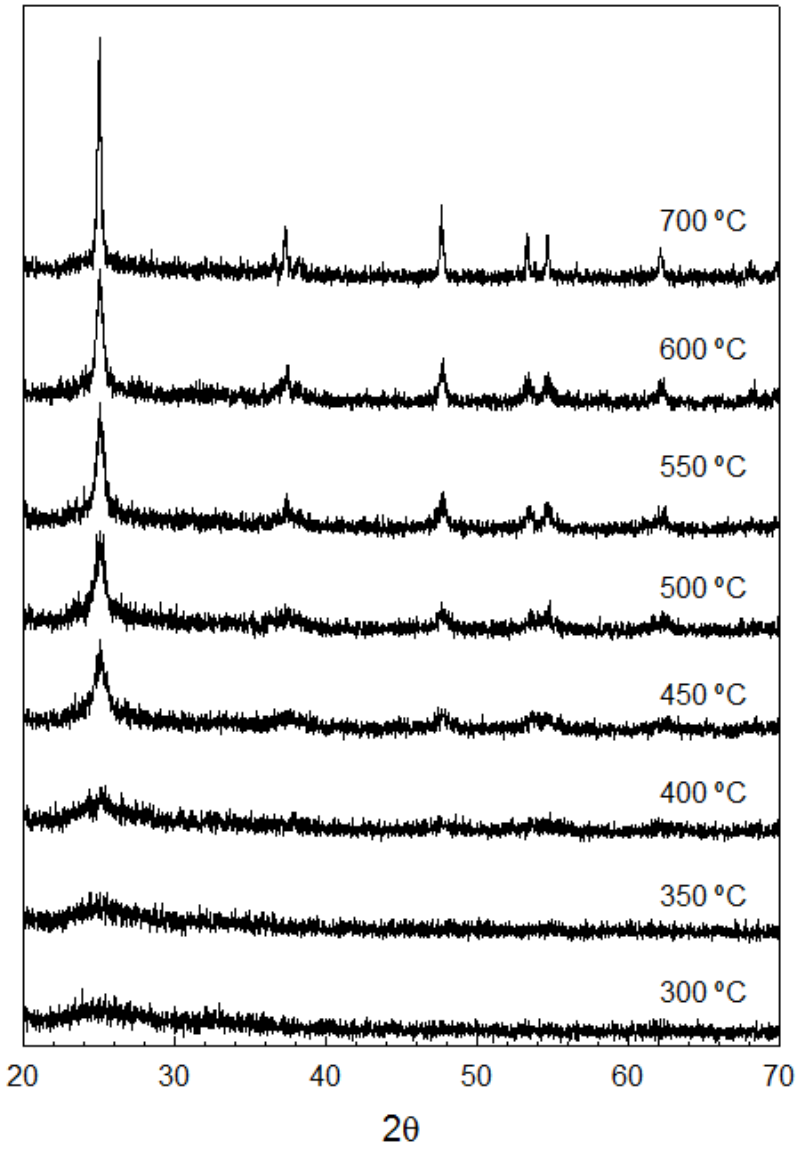

Figure 6. XRD pattern of TiO_2_1:1.6 as a function of temperature

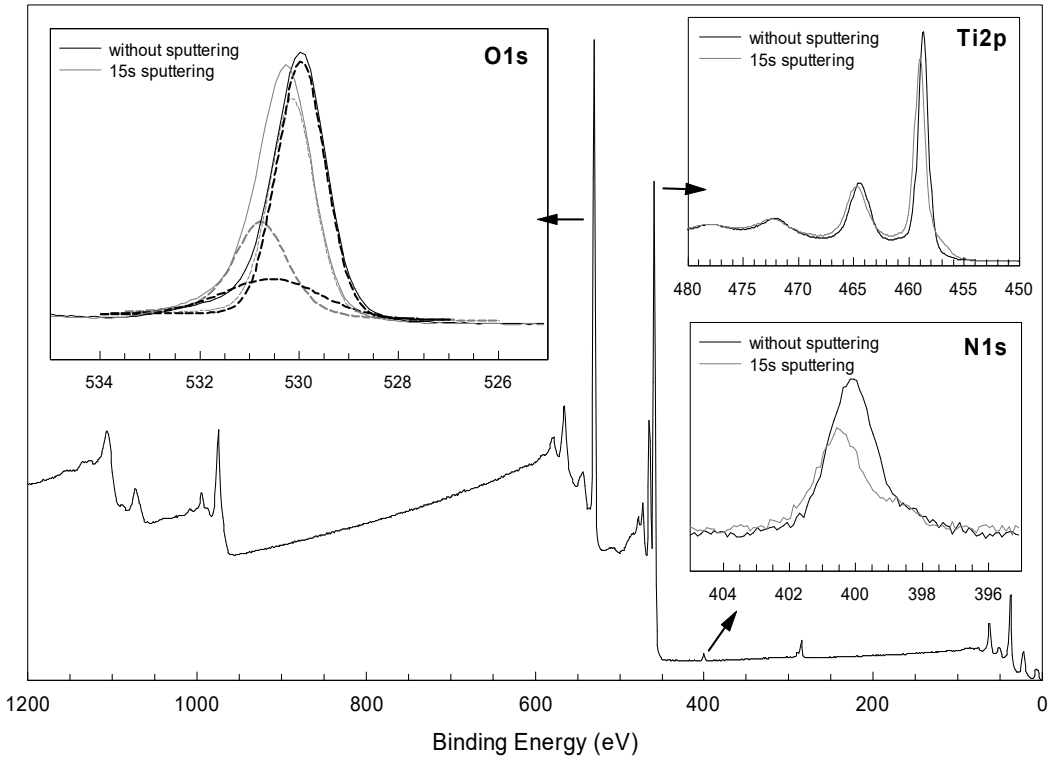

Figure 7. XPS of fresh TiO_2_1:1.6 catalyst.

1

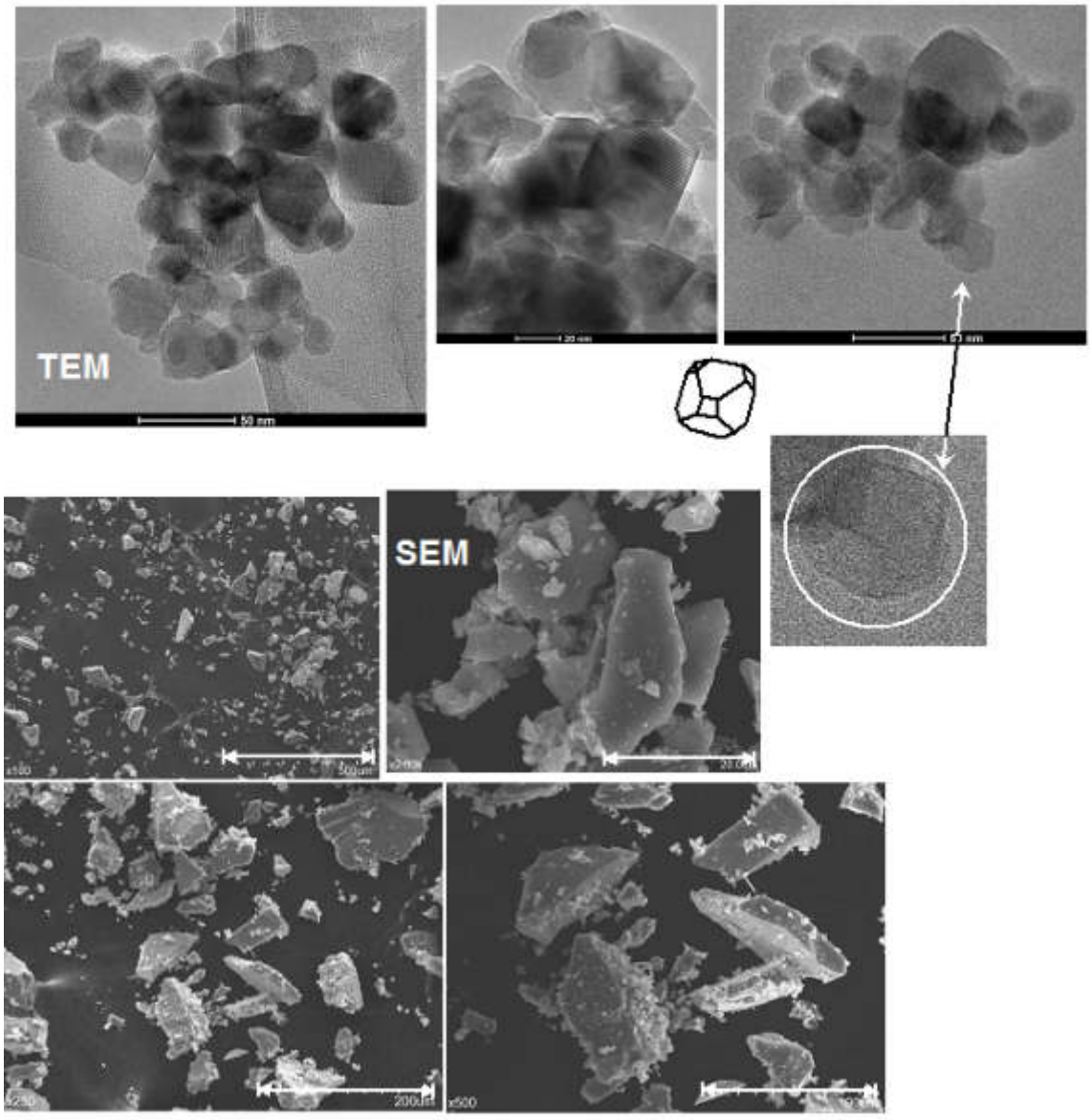

Figure 8. SEM/TEM of fresh TiO_2_1:1.6 catalyst.

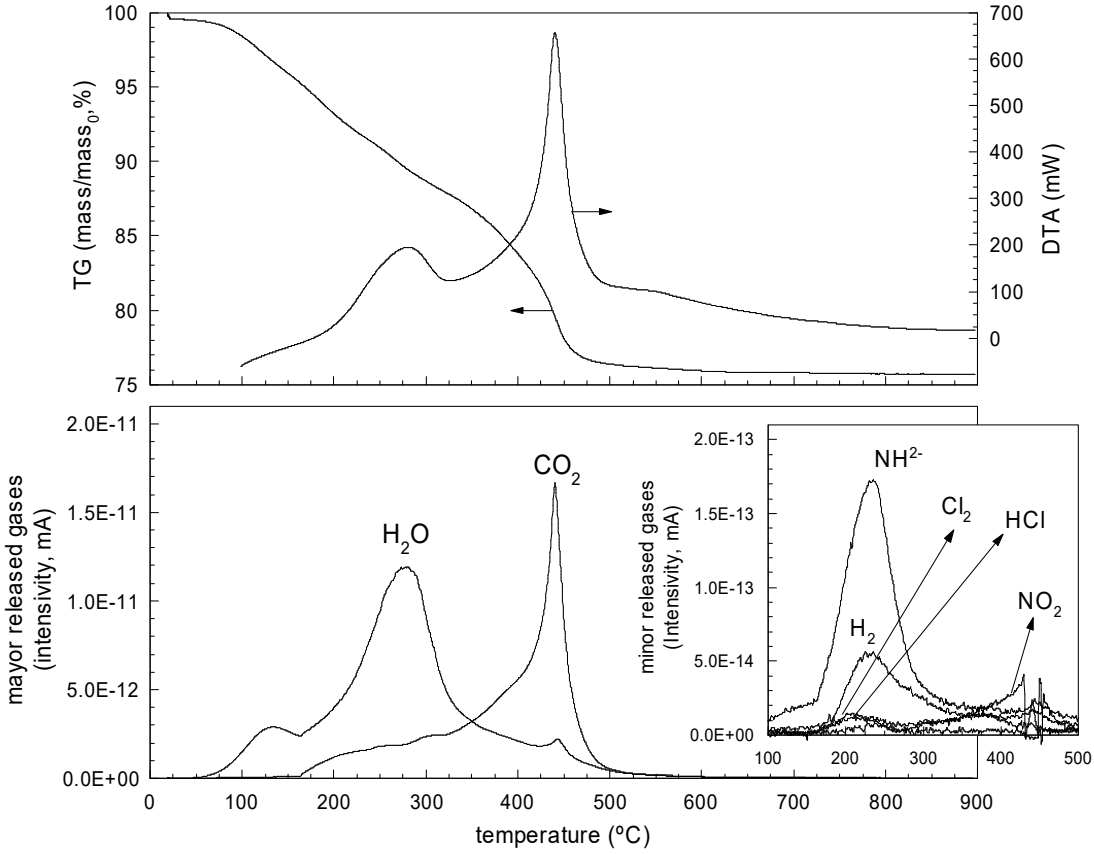

Figure 9. TG-DTA-MS of fresh TiO_2_1:1.6 catalyst.

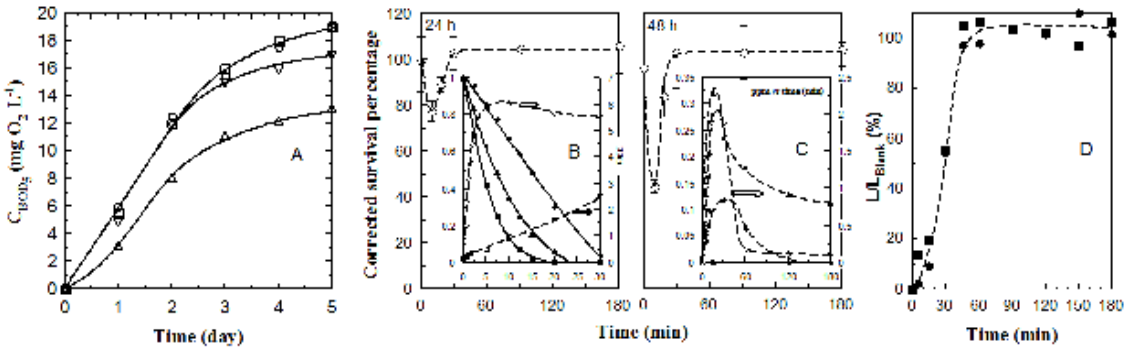

Figure 10. Black light photocatalytic ozonation of a mixture of clopyralid, picloram and triclopyr. Experimental conditions: T = 20 ºC, V = 1.0 L; I = $6.86 \cdot 10^{-5}$ Einstein min^{-1} L^{-1}; pH = 4.0 (average value), $C_{herbicide}$ = 5.0 ppm (each). $C_{Catalyst}$= 0.5 g L^{-1} TiO_2_1:1.6.

A. BOD evolution in synthetic water: O, water without herbicides ; □, doped water with 5 ppm in each herbicide; Δ, doped water after 10 min of photocatalytic ozonation; ∇, doped water after 180 min of photocatalytic ozonation.

B. 24 h *D. Parvula* survival percentage after different periods of photocatalytic ozonation. (Embedded figure: evolution of ●, clopyralid, ■, picloram, ▲, triclopyr, O, chloride, and □, nitrate during the experiment).

C. 48 h *D. Parvula* survival percentage after different periods of photocatalytic ozonation. (Embedded figure: evolution of ●, acetic acid, ○, propionic acid, and ▲, oxalic acid during the experiment).

D. Fotoxicity evolution of black light photocatalytic ozonation of a mixture of clopyralid, picloram and triclopyr. ●, *L. Sativa*; ■, *S. Lycopersicum*